

# External Electric Field Effects on Fluorescence of Pyrene Butyric Acid in a Polymer Film: Concentration Dependence and Temperature Dependence

Anjue Mane Ara, Toshifumi Iimori, Tomokazu Yoshizawa, Takakazu Nakabayashi, and Nobuhiro Ohta\*

Research Institute for Electronic Science, Hokkaido University, Sapporo 060-0812, Japan

Received: June 21, 2006; In Final Form: August 21, 2006

Fluorescence spectra and electrofluorescence spectra (plots of the electric field-induced change in fluorescence intensity as a function of wavelength) have been measured at different temperatures for pyrene butyric acid (PBA) in a PMMA film at different concentrations. At a low concentration of 0.5 mol % where fluorescence emitted from the locally excited state of PBA (LE fluorescence) is dominant, LE fluorescence spectra show only the Stark shift in the presence of an electric field ( $F$ ), which results from the difference in molecular polarizability between the ground and emitting states. At a high concentration of 10 mol % where the so-called sandwich-type excimer fluorescence (EX(1)) is dominant, both EX(1) and LE fluorescence are quenched by  $F$ . Another fluorescence assigned to a partially overlapped excimer (EX(2)) also exists at room temperature, and this emission is enhanced by  $F$ . As the temperature decreases, three fluorescence emissions whose electric field effects are different from each other become clear besides EX(1) and LE fluorescence, indicating that at least five fluorescence components exist at high concentrations at low temperatures. At a medium concentration of 5 mol % where EX(1) is comparable in intensity to the LE fluorescence, the intensity of EX(1) is not affected by  $F$  at any temperature, but LE fluorescence and EX(2) are markedly influenced by  $F$  at room temperature, and four fluorescence emissions are confirmed at low temperatures.

## 1. Introduction

Fluorescent probes have been widely employed as sensors for the distinct fields of study.<sup>1,2</sup> Among many fluorescence probes, pyrene and some of its derivatives have attracted special attention because of their valuable photophysical properties such as high fluorescence quantum yield, long fluorescence lifetime, high solvent polarity dependence of the vibrational structure of fluorescence spectra, and high ability for excimer formation.<sup>3–6</sup> These characteristics of pyrene and its derivatives are suitable for the application as a sensor to microscopically probe an environment around the molecules under study.

Among fluorescent probes of the pyrene family, pyrene butyric acid, hereafter denoted as PBA, has been in particular used to probe the microscopic environment at the inside of biological macromolecules such as proteins, micelles, vesicles, or lipids, since PBA has amphiphilicity arising from the carboxyl group and the aromatic ring, oxygen sensing property, and the capability of not only excimer formation but also hydrogen bonding.<sup>5–10</sup> In fact, PBA has advantages in the sense that it shows a selective affinity for a unique site of the macromolecules and reflects the nature of the surrounding environments in the emission properties.<sup>5,6,11–14</sup>

It is known that a strong electrostatic field caused by polar functional groups exists in living cells and proteins, and it has been reported that these electrostatic fields play a significant role in reactions in biological systems. Not only in biological macromolecules, but also in a simple solution, a strong electrostatic field exists; molecules dissolved in solution are in the strong electrostatic field caused by solvation, which is also important as a solvent effect in chemical reaction. Therefore,

the assessment of these electrostatic fields is important, and this may be possible by using a fluorescence probe such as PBA in a variety of surroundings. For that purpose, electric field effects on fluorescence intensity as well as on fluorescence spectra must be elucidated. In fact, strong electric field effects on fluorescence are expected for PBA, since significant effects have been observed even in nonpolar molecules of pyrene, i.e., in parent molecules of PBA, at high concentrations where excimer fluorescence is observed. Further, the study of the electric field effects on the emission of PBA is important not only for the assessment of this molecule as the fluorescence probe of the environmental surroundings, but also for the elucidation of both excimer formation dynamics of this molecules and its electric field dependence.

As preliminarily reported in our previous paper,<sup>15</sup> fluorescence spectra as well as electrofluorescence spectra of pyrene embedded in a poly(methyl methacrylate) (PMMA) film show a remarkable temperature dependence at high concentrations where fluorescent excimer is formed. It was suggested that the temperature dependence of the electric field effects of fluorescence would give information about the potential surface of various excimer species and their excitation dynamics. Similarly, it is expected that detailed information about different species of excimer of PBA can be obtained, based on the experiments of the temperature dependence of the emission spectrum of PBA and its electric field effects.

In the present study, electric field effects on fluorescence spectra of PBA embedded in a PMMA matrix have been examined at low, medium, and high concentrations of 0.5, 5, and 10 mol %, respectively, at various temperatures in the range of 40–295 K. At room temperature, a partially overlapped excimer fluorescence contributes to the electrofluorescence

\* Address correspondence to this author. E-mail: nohta@es.hokudai.ac.jp.

spectrum besides the monomer fluorescence and the fully overlapped excimer fluorescence. At low temperatures, new species of partially overlapped excimer which are distinct from the one observed at room temperature appear, and it is shown that the electric field effects on fluorescence of these excimer components are different from each other.

## 2. Experimental Section

Pyrene butyric acid (PBA) was purified by crystallization from ethanol. PMMA was purified by precipitation with methanol and benzene. The experimental apparatus used for the measurements of the electroabsorption and electrofluorescence spectra at different temperatures and the sample preparation of PBA embedded in a PMMA film are the same as the ones reported in our previous papers.<sup>15–17</sup> The concentration of PBA was determined by using the following equation:  $a = [(x/M)/(x/M + k/M')] \times 100$ , where  $a$  is the concentration of PBA relative to the monomer unit of PMMA,  $x$  and  $M$  are the amount and the molecular weight of PBA, respectively, and  $k$  and  $M'$  are the amount and the molecular weight of PMMA, respectively. Note that the molecular weight of the monomer unit of PMMA is 100. At first, 0.04 g of PMMA was dissolved into 2 mL of chloroform. Then,  $5.79 \times 10^{-4}$ ,  $0.61 \times 10^{-2}$ , and  $1.28 \times 10^{-2}$  g of PBA were dissolved into the above-mentioned chloroform solution of PMMA to prepare 0.5, 5, and 10 mol % PBA in PMMA, respectively. A certain amount of chloroform solution of PBA and PMMA was poured onto an ITO-coated quartz substrate, and a thin polymer film of PMMA doped with PBA was prepared by a spin coating method. Then, a semi-transparent aluminum (Al) film was deposited on the dried polymer film by using a vacuum vapor deposition method. The ITO and Al films were used as electrodes. Hereafter, the applied electric field is denoted by  $F$ , and its strength is represented in rms. The thickness of the polymer film was typically  $0.6 \mu\text{m}$ , and the strength of the applied electric field, which was calculated from the applied voltage divided by the film thickness, was typically  $1 \text{ MV cm}^{-1}$ . All the optical measurements were carried out under vacuum conditions.

Using electric field modulation spectroscopy, we measured electric-field-induced changes in absorption and fluorescence spectra and obtained the electroabsorption and electrofluorescence spectra as a function of wavelength. A sinusoidal ac voltage was applied to a sample with a modulation frequency of 40 Hz. Field-induced change in transmitted excitation light intensity ( $\Delta I$ ) or in fluorescence intensity ( $\Delta I_F$ ) was detected with a lock-in amplifier (SR830, SRS) at the second harmonic of the modulation frequency; the field-induced change in intensity, which is proportional to the square of the applied field strength, was obtained. A dc component corresponding to the total intensity of the transmitted excitation light ( $I$ ) or fluorescence,  $I_F$ , was simultaneously measured at each wavelength. Note that the field-induced change in absorption intensity ( $\Delta A$ ) was obtained from  $-\Delta I$  divided by  $2.303I$ .<sup>18</sup>  $\Delta I_F$  corresponds to the difference between  $I_F$  at  $F$  and  $I_F$  at zero field at each wavelength, i.e.,  $\Delta I_F = I_F(F \neq 0) - I_F(F = 0)$ . Since  $I_F(F = 0) \gg \Delta I_F$  at any wavelength, fluorescence and electrofluorescence spectra could be simultaneously obtained by monitoring the dc component of the fluorescence intensity and the ac component synchronized with the modulated applied electric field, respectively.

In the low-temperature measurements, the sample substrate was cooled by using a cryogenic refrigerating system (Daikin, V202CSLR) equipped with quartz optical windows, and the temperature ( $T$ ) of the substrate was monitored by using a

temperature controller (Scientific Instruments, model 9600) with a silicone diode thermometer (Scientific Instruments, Si410A).<sup>15</sup> The substrate was excited from the semitransparent aluminum side, and an incident angle of the excitation light to the substrate was  $\sim 45^\circ$ .

## 3. Theoretical Background

When an electric field is applied to molecules, each energy level is shifted, and the magnitude of each shift depends on the electric dipole moment ( $\mu$ ) and the molecular polarizability ( $\alpha$ ) of the state concerned; the level shift is given by  $-\mu F - \alpha F^2/2$ . As a result, the transition energy for absorption as well as for emission changes in the presence of  $F$ . For an isotropic and immobilized sample, the presence of  $F$  will broaden the transition energy due to the change in electric dipole moment following absorption or emission, giving rise to a Stark effect line shape that is approximately the second derivative of the absorption (emission) spectrum.<sup>18</sup> If the change in molecular polarizability following photoexcitation is significant, the Stark effect line shape is the first derivative of the absorption (emission) spectrum. If the transition moment is affected by  $F$ , the Stark effect line shape is the same as the absorption (emission) spectrum.

By assuming that the original isotropic distribution is maintained even in the presence of  $F$ , the change in absorbance at frequency ( $\nu$ ) may be given by the following equation:<sup>18–20</sup>

$$\Delta A(\nu) = (fF)^2 \left[ AA(\nu) + B\nu \frac{d}{d\nu} \left( \frac{A(\nu)}{\nu} \right) + C\nu \frac{d^2}{d\nu^2} \left( \frac{A(\nu)}{\nu} \right) \right] \quad (1)$$

where  $f$  is the internal field factor. The coefficient  $A$  depends on the transition moment polarizability and hyperpolarizability, and  $B$  and  $C$  are given as follows:

$$B = [\Delta\bar{\alpha}/2 + (\Delta\alpha_m - \Delta\bar{\alpha})(3\cos^2\chi - 1)/10]/(hc) \quad (2)$$

$$C = (\Delta\mu)^2[5 + (3\cos^2\xi - 1)(3\cos^2\chi - 1)]/(30h^2c^2) \quad (3)$$

where  $h$  and  $c$  represent Planck's constant and light speed, respectively. Here,  $\Delta\mu$  and  $\Delta\alpha$  are the differences in electric dipole moment and molecular polarizability, respectively, between the ground state (g) and the excited state (e), i.e.,  $\Delta\mu = \mu_e - \mu_g$ , and  $\Delta\alpha = \alpha_e - \alpha_g$ :

$$\Delta\mu = |\Delta\mu|; \quad \Delta\bar{\alpha} = (1/3) \text{Tr}(\Delta\alpha) \quad (4)$$

$\Delta\alpha_m$  denotes the diagonal component of  $\Delta\alpha$  with respect to the direction of the transition dipole moment,  $\chi$  is the angle between the direction of  $F$  and the electric vector of the excitation light, and  $\xi$  is the angle between the direction of  $\Delta\mu$  and the transition dipole moment. The value of  $\Delta\mu$  or  $\Delta\bar{\alpha}$  can be easily obtained from the analysis of the derivative parts of the electroabsorption spectra.

Similarly, the field-induced change in fluorescence intensity at frequency observed at the second harmonic of the modulation frequency in a polymer film can be given by the following equation:

$$\Delta I_F(\nu) = (fF)^2 \left[ A'I_F(\nu) + B'\nu^3 \frac{d}{d\nu} \left( \frac{I_F(\nu)}{\nu^3} \right) + C'\nu^3 \frac{d^2}{d\nu^2} \left( \frac{I_F(\nu)}{\nu^3} \right) \right] \quad (5)$$

The first and the second derivative components correspond to the spectral shift and the spectral broadening resulting from the

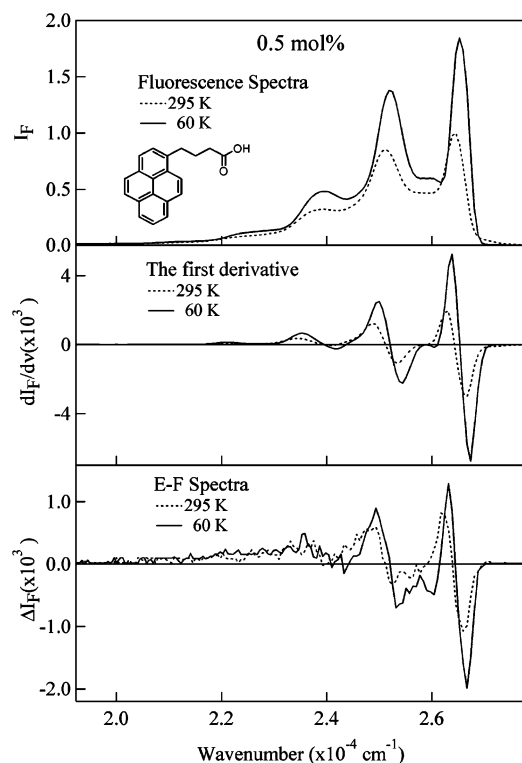


**Figure 1.** Fluorescence spectrum (top), the first derivative of the fluorescence spectrum (middle), and E-F spectrum (bottom) of PBA at a concentration of 0.5 mol % in a PMMA film observed at 295 K (dotted line) and at 60 K (solid line). The applied field strength was  $1.0 \text{ MV cm}^{-1}$ . The maximum fluorescence intensity at 295 K is normalized to unity.

difference in molecular polarizability and electric dipole moment between the fluorescent state and the ground state, respectively.<sup>18</sup>

Absorption intensity as well as fluorescence intensity may increase or decrease in the presence of  $F$ . In such a case, the zeroth derivative component is not zero in eq 1 or eq 5. The field-induced change in absorption intensity and in fluorescence intensity can be attributed to the field-induced change in transition moment and in fluorescence quantum yield, respectively, if molecular orientation is not concerned.

#### 4. Results and Discussion

Absorption, electroabsorption, fluorescence, and electrofluorescence spectra of PBA doped in a PMMA film have been measured at different temperatures. The following concentrations of PBA relative to the monomer unit of PMMA were used as the representatives of low, medium, and high concentrations, respectively, i.e., 0.5, 5, and 10 mol %. A notable temperature dependence was not observed in absorption as well as in electroabsorption spectra of PBA except for a slight shift of the spectra. On the other hand, remarkable temperature dependence was observed in fluorescence as well as in electrofluorescence spectra. Hereafter, the electrofluorescence spectrum is abbreviated as E-F spectrum.

**4.1. At a Low Concentration of 0.5 mol %.** Fluorescence spectra and E-F spectra of PBA in a PMMA film at a concentration of 0.5 mol % observed at  $T = 295$  and 60 K are shown in Figure 1. The applied field strength was  $1.0 \text{ MV cm}^{-1}$ . Excitation was done at the wavelengths where the field-induced change in absorption intensity was negligible. The observed fluorescence spectra, which show a well-defined vibrational structure, are assigned as the spectra of the fluorescence emitted

from the locally excited state of PBA (denoted by LE fluorescence). At a low concentration of 0.5 mol %, therefore, the interaction among PBA molecules is negligible, and the LE fluorescence is regarded as the fluorescence of the PBA monomer. The shape of the E-F spectrum at a low concentration of 0.5 mol % is essentially the same as the first derivative of the fluorescence spectrum (see Figure 1), indicating that the field-induced change in fluorescence spectrum comes from the change in molecular polarizability following emission and that the fluorescence decay rate is not affected by an electric field.<sup>18</sup> As shown in Figure 1, fluorescence spectra as well as E-F spectra at 0.5 mol % are essentially independent of the temperature, as far as the spectral shape is concerned. It is also worth mentioning that the fluorescence intensity as well as the intensity of the E-F spectra increases as the temperature decreases. This is probably because the nonradiative decay rate at the emitting state of the LE fluorescence becomes smaller with the decrease of the temperature. Hereafter, LE fluorescence is denoted as LE-F.

**4.2. At a High Concentration of 10 mol %.** Fluorescence and E-F spectra of PBA in a PMMA film at a concentration of 10 mol % observed at different temperatures with a field strength of  $1.0 \text{ MV cm}^{-1}$  are shown in Figure 2. The fluorescence spectra are dominated by a broad emission with a peak at  $21\,280 \text{ cm}^{-1}$  ( $\sim 470 \text{ nm}$ ), but a weak fluorescence emitted from the locally excited state of PBA, i.e., LE-F, still exists. The broad emission is assigned as the fluorescence of excimer that has a sandwich-type structure. Hereafter, this emission is called EX(1). The absorption spectra of PBA at 10 mol % are very different from the ones for pyrene crystals, indicating that PBA is randomly distributed in PMMA without crystal formation. In the whole temperature range, EX(1) maintains its broad structureless feature.  $I_F$  at  $25\,000 \text{ cm}^{-1}$  increases with a decrease of temperature, indicating that emission other than LE-F or EX(1) increases. The EX(1) spectrum was subtracted from the observed emission spectra. The results are shown in Figure 3a. It is noted that the fluorescence spectrum of EX(1) used for the subtraction was regarded as given by a superposition of two Gaussian profiles, with which the fluorescence spectral shape in the region lower than  $22\,200 \text{ cm}^{-1}$  was reproduced quite well in every case; the peak of the Gaussian profiles is at  $20\,911$  ( $4416$ ) and  $21\,660$  ( $1487$ )  $\text{cm}^{-1}$  at 295 K and at  $20\,990$  ( $4085$ ) and  $21\,306$  ( $867$ )  $\text{cm}^{-1}$  at 75 K, where the full width at half-maximum is shown in parentheses (in units of  $\text{cm}^{-1}$ ). As the temperature decreases, the former peak, which is much stronger than the latter in every temperature, is blue-shifted, while the latter is red-shifted. As the temperature decreases further, the bandwidth becomes smaller in both profiles. The extracted emission spectrum at a low temperature of 75 or 100 K shown in Figure 3a is very similar to the V-luminescence observed in a supercooled crystal of pyrene<sup>21–23</sup> and to the B-fluorescence observed at low temperatures in a microcrystalline film of pyrene.<sup>24</sup> Except for the high wavenumber region where fluorescence is superimposed by LE-F, the extracted spectrum at 75 K is reproduced by a superposition of two Gaussian profiles with a peak at  $25\,220 \text{ cm}^{-1}$  ( $\sim 396 \text{ nm}$ ) and at  $24\,040 \text{ cm}^{-1}$  ( $\sim 415 \text{ nm}$ ), denoted by  $b_{\text{LT}}(\text{I})$  and  $b_{\text{LT}}(\text{II})$ , respectively (see Figure 4a). The intensity of the broad emission simulated by a sum of  $b_{\text{LT}}(\text{I})$  and  $b_{\text{LT}}(\text{II})$  significantly increases as the temperature decreases.

Plots of the  $I_F$  as a function of temperature show that fluorescence at  $\sim 400 \text{ nm}$  monotonically increases with lowering temperature, as shown in Figure 5a. On the other hand,  $I_F$  at  $21\,280 \text{ cm}^{-1}$  ( $470 \text{ nm}$ ), which corresponds to EX(1), is not so

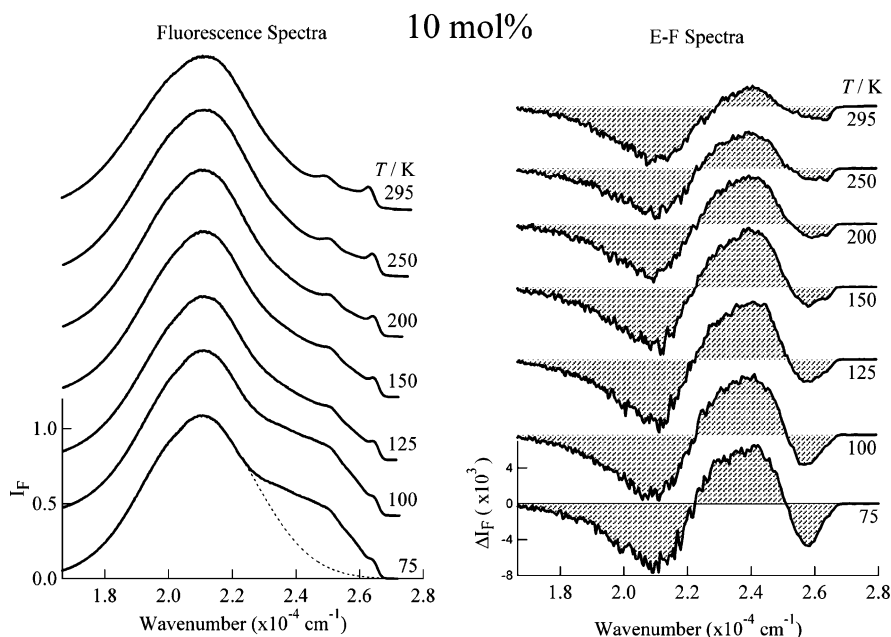


**Figure 2.** Temperature dependence of the fluorescence spectra (left) and the E-F spectra (right) of PBA at a concentration of 10 mol % in a PMMA film. Temperature is shown in each spectrum. Applied field strength was  $1.0 \text{ MV cm}^{-1}$ . The dotted line shows the simulated spectrum of a sandwich-type excimer fluorescence, i.e., EX(1).

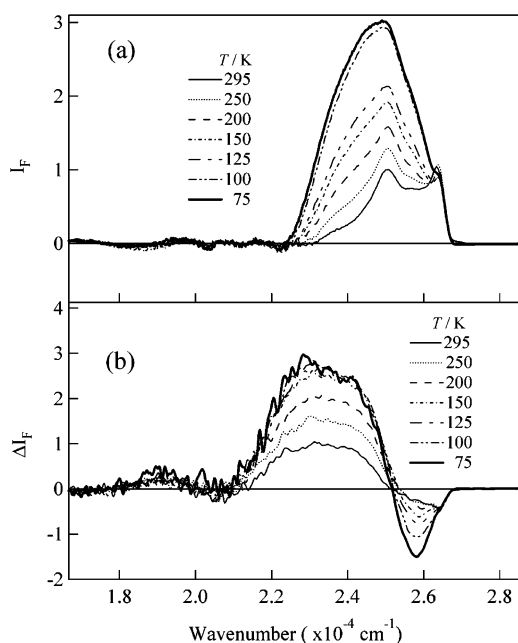


**Figure 3.** Temperature dependence of the extracted fluorescence spectrum (a) and extracted E-F spectrum (b) of PBA at 10 mol % in a PMMA film. The contribution of EX(1) is subtracted from the observed spectrum. See the text about the procedure of the subtraction.

influenced by a change in temperature. Actually, EX(1) becomes a little stronger as the temperature decreases from 295 to 250 K. Below 250 K, on the other hand, EX(1) becomes a little weaker as the temperature decreases.  $I_F$  at  $23\,000 \text{ cm}^{-1}$  ( $435 \text{ nm}$ ) shows the temperature dependence which is similar to that of the emission at  $25\,000 \text{ cm}^{-1}$ ; a small increase in  $I_F$  was observed as the temperature decreases (see Figure 5a).

E-F spectra at 10 mol % show a remarkable temperature dependence particularly in the wavenumber region above  $22\,000 \text{ cm}^{-1}$ , as shown in Figure 2. E-F spectra clearly show that LE-F is quenched by  $F$  at 295 K and that EX(1) at 10 mol % shows a significant field-induced quenching in the whole temperature range. As the temperature decreases, a sharp negative band

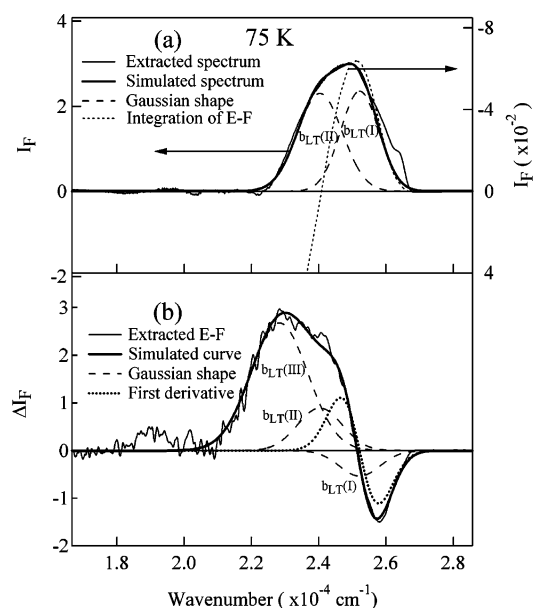


**Figure 4.** (a) Extracted fluorescence spectrum at 75 K (thin solid line), simulated spectrum (thick solid line) by a sum of two bands having a Gaussian profile, i.e.,  $b_{LT(I)}$  and  $-b_{LT(II)}$  (broken line), the integration of the E-F spectrum made from the high wavenumber side (dotted line), (b) extracted E-F spectrum at 75 K (thin solid line), three bands with a Gaussian shape, i.e.,  $b_{LT(I)}$ ,  $-b_{LT(II)}$ , and  $-b_{LT(III)}$  (broken line), the first derivative of  $b_{LT(I)}$  (dotted line), and the simulated spectrum (thick solid line).

appears in the spectral region of LE-F. The peak of the negative band in the E-F spectra is located at  $25\,840 \text{ cm}^{-1}$  ( $387 \text{ nm}$ ) below 150 K, and this band cannot be attributed to LE-F. The E-F spectrum of EX(1) was subtracted from the E-F spectra observed at each temperature by assuming that the E-F spectrum of EX(1) has the same shape as the fluorescence spectrum of EX(1). The results are shown in Figure 3b. The validity of the assumption is confirmed from the fact that the extracted spectra in Figure 3b show nearly zero intensity in the wavenumber region below  $21\,000 \text{ cm}^{-1}$ , indicating that spectral shift and broadening appeared as the derivative components of the



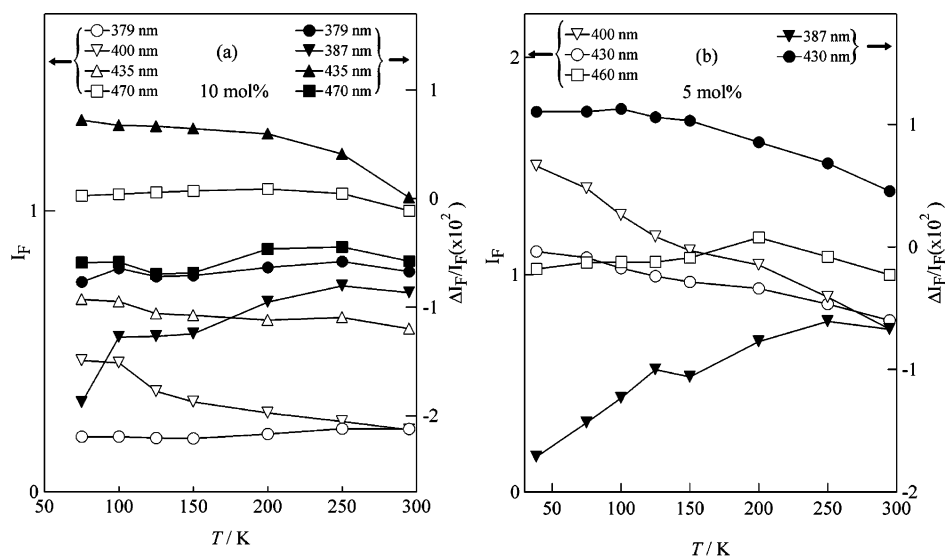


**Figure 5.** Plots of the fluorescence intensity ( $I_F$ ) of PBA and its field-induced change ( $\Delta I_F$ ) relative to  $I_F$  monitored at different wavelengths as a function of temperature at 10 (left) and at 5 mol % (right).  $I_F$  and  $\Delta I_F/I_F$  are shown in the scale of the left- and right-hand sides, respectively.

emission spectrum are negligible for EX(1). It is interesting that  $\Delta\mu$  or  $\Delta\alpha$  is very small between the fluorescent state and the ground state of EX(1). It may be worth mentioning that the same assumption is applicable for the sandwich-type excimer fluorescence of pyrene in a PMMA film.<sup>16</sup>

As shown in Figure 3a, LE-F is quite clear at high temperatures. As the temperature decreases, the emission located in the wavenumber region lower than that of LE-F, which has a peak at  $\sim 25\,000\text{ cm}^{-1}$ , is enhanced and shows a remarkable electric field effect (see Figure 3). As a result, the E-F spectrum as well as the emission spectrum of LE-F becomes unclear at low temperatures. LE-F increases a little with the decrease of temperature from 295 to 250 K, while LE-F decreases with the further decrease of the temperature. With respect to the electric field effect, LE-F seems to be nearly independent of temperature. The temperature dependence of  $\Delta I_F$  relative to  $I_F$ , which was obtained by monitoring the emission at 379, 387, 435, and 470 nm, respectively, is shown in Figure 5a.

The temperature dependence of the E-F spectra of PBA at 10 mol % is summarized as follows:

(1) A field-induced quenching of LE-F, which is nearly independent of the temperature, occurs at high concentrations.  
 (2) E-F spectra at wavelengths longer than 470 nm show nearly the same shape as the fluorescence spectra with a negative value, indicating that EX(1) is quenched by  $F$ . The magnitude of the quenching of EX(1) is roughly independent of the temperature.

(3) E-F spectra show a sharp negative peak at  $25\,840\text{ cm}^{-1}$  (387 nm) at low temperatures. The magnitude of the quenching at 387 nm remarkably and monotonically increases as the temperature decreases especially below 150 K.

(4) E-F spectra show a broad positive band in the region of  $22\,000\text{--}25\,300\text{ cm}^{-1}$  (395–450 nm), and the intensity of this band increases as the temperature decreases.

At room temperature, PBA in a PMMA film seems to show three components of fluorescence at high concentrations, as in the case of pyrene: LE-F, EX(1), and partially overlapped excimer fluorescence (EX(2)). The emission spectrum of EX(2) was derived by assuming that the E-F spectra at room temperature are given by a linear combination of LE-F, EX(1), and EX(2) and that the emission spectrum at 10 mol % at room temperature is given by a sum of LE-F and EX(1). The validity of the assumption was shown in pyrene.<sup>16</sup> The EX(2) spectrum

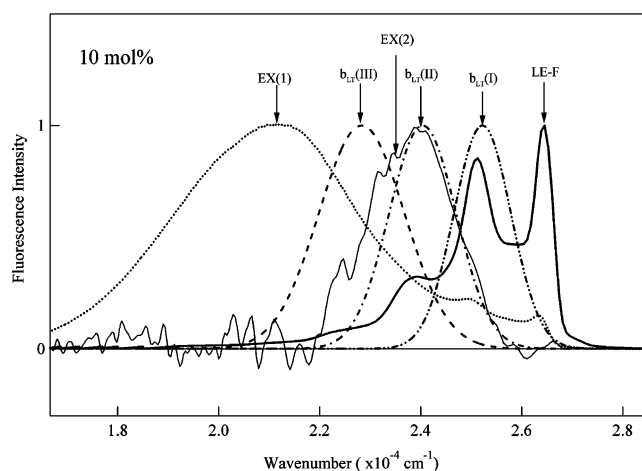


**Figure 6.** Fluorescence spectra of PBA at 0.5 (thick solid line) and 10 mol % (dotted line) dominated by LE-F and by EX(1), EX(2) spectrum at room temperature (thin solid line), and  $b_{LT}(I)$ ,  $-(II)$ ,  $-(III)$  spectra at low temperatures (double chain line, chain line, and broken line, respectively).

at room temperature thus obtained is shown in Figure 6. The field-induced quenching of LE-F can be ascribed to the field-induced acceleration of the nonradiative process in the  $S_1$  state, which comes from the field-induced increase of the formation rate of the sandwich-type excimer. In analogy from the time-resolved measurements of the electric field effects on fluorescence decay of pyrene,<sup>25</sup> the field-induced quenching of EX(1) of PBA probably comes from the field-induced increase in nonradiative decay rate at the emitting state of EX(1), and the field-induced enhancement of EX(2) probably comes from a field-induced increase in the initial population of the partially overlapped excimer. The increase in the initial population of EX(2) may be ascribed to the field-induced increase in stability of the rather unstable excimer.

The sharp negative band with a peak at  $26\,000\text{ cm}^{-1}$  (387 nm) observed in the E-F spectra at low temperatures is attributed to a new species that exists only at low temperatures. There is no doubt that the broad emission with a peak at  $24\,940\text{ cm}^{-1}$  ( $\sim 400\text{ nm}$ ) newly appears as the temperature decreases (see Figure 3a). The E-F spectra suggest that the extracted emission spectrum shown in Figure 4a is a superposition of two excimer fluorescence emissions having different responses to the applied

electric field from each other, i.e.,  $b_{LT}(I)$  and  $b_{LT}(II)$ . The extracted E-F spectrum in the high wavenumber region is very similar to the first derivative of  $b_{LT}(I)$  (see Figure 4b). Actually, the extracted E-F spectrum where the E-F spectrum of EX(1) was subtracted can be decomposed into the bands, each of which can be expressed by a Gaussian shape, denoted by  $b_{LT}(II)$ ,  $b_{LT}(III)$ , and the band given by a linear combination of  $b_{LT}(I)$  and its first derivative, as shown in Figure 4b. Note that the peak positions of  $b_{LT}(I)$ ,  $- (II)$ ,  $- (III)$  are 400, 415, and 430 nm, respectively.

The presence of the first derivative component of the  $b_{LT}(I)$  is confirmed in the E-F spectra since the integrated spectrum of the E-F spectrum in the high wavenumber region well reproduces  $b_{LT}(I)$  (see Figure 4a). The fact that  $b_{LT}(II)$  was not reproduced by the integration of the E-F spectrum implies that  $b_{LT}(II)$  does not come from the vibronic structure starting from  $b_{LT}(I)$  and that  $b_{LT}(I)$  and  $b_{LT}(II)$  are assigned to the ones emitted from different species from each other;  $b_{LT}(I)$  and  $b_{LT}(II)$  are fluorescence emissions which are assigned to different species of excimer from each other. As the temperature decreases,  $b_{LT}(III)$  becomes stronger in the extracted E-F spectrum (see Figures 3b and 4b), but the corresponding emission band is not confirmed in the extracted fluorescence spectra shown in Figure 4a. In contrast with  $b_{LT}(III)$ ,  $b_{LT}(II)$  was found both in the extracted E-F spectra and in the extracted fluorescence spectra at low temperatures, as shown in Figure 4a,b. The peak position of  $b_{LT}(II)$ , i.e., 415 nm, is nearly the same as that of EX(2) observed at room temperature, but the remarkable field-induced enhancement of EX(2) at room temperature is similar to that of  $b_{LT}(III)$  observed at low temperatures.

As mentioned above, PBA in a PMMA film shows five fluorescence components at high concentration (10 mol %) and at low temperatures, i.e., LE-F, sandwich-type excimer fluorescence (EX(1)), and fluorescence components characterized by  $b_{LT}(I)$ ,  $- (II)$ , and  $- (III)$ , respectively. The fluorescence spectra of these components are summarized in Figure 6. The  $b_{LT}(III)$  may correspond to EX(2) confirmed at room temperature in the sense that both EX(2) and  $b_{LT}(III)$  show a remarkable field-induced enhancement, though the peak position of  $b_{LT}(III)$  is located at a lower wavenumber than EX(2). LE-F and EX(1) are quenched by  $F$  at any temperature.  $b_{LT}(I)$ , which shows both Stark shift and field-induced quenching, is markedly enhanced with a lowering temperature. By analyzing the Stark shift, the magnitude of the change in molecular polarizability following the emission of  $b_{LT}(I)$  is estimated to be about  $124 \text{ \AA}^3$  with a Lorentz field correction.<sup>26</sup>  $b_{LT}(II)$ , which increases a little in the presence of  $F$ , becomes stronger as the temperature decreases.

The characterization of the emitting state of the V-luminescence or B-fluorescence of pyrene, whose spectrum is very similar to the extracted emission spectrum shown in Figure 4a, is somewhat controversial, but these emissions have been ascribed to the excimer species having a partially overlapped conformation. The presence of the excimer, which has a partially overlapped conformation in pyrene and its derivatives, has been pointed out in other systems, and the fluorescence spectrum of this species has been reported to be located in the region of 400–420 nm in a vapor-deposited film,<sup>27</sup> at 400 nm in a single crystal,<sup>28</sup> at 420 nm in a pyrene-labeled polymer<sup>2</sup> and in a LB film,<sup>29</sup> at 415 nm in a PMMA matrix,<sup>16</sup> in neat liquid,<sup>30</sup> and in amorphous silica glass.<sup>31</sup> The present results show that there are at least three fluorescence components emitted from the distinct states of the partially overlapped excimer at 10 mol %:  $b_{LT}(I)$ ,  $- (II)$ , and  $- (III)$ . An implication of the crystal spectroscopy

is consistent with a model that there are several potential minima due to differently overlapped conformations in the excited state. In a pyrene crystal, the nearest neighbor pyrene molecules are in a parallel-displaced configuration.<sup>2</sup> A theoretical model taking both the nearest and the next-nearest pairs into account has attempted to interpret the fully relaxed excimer, i.e., sandwich-type excimer (EX(1)), and the partially overlapped excimer that originates from the corresponding two intermolecular interactions.<sup>32</sup> Hence, it will be pertinent to consider that the distinct states detected in this experiment, i.e., emitting states of  $b_{LT}(I)$ ,  $- (II)$ , and  $- (III)$ , are due to potential minima corresponding to different conformations of excimer in a PMMA polymer film. As mentioned above,  $b_{LT}(I)$  is quenched by  $F$ , while  $b_{LT}(II)$  is a little enhanced by  $F$  and  $b_{LT}(III)$  is largely enhanced by  $F$ .

At room temperature, one of the potential minima, namely one particular conformation of partially overlapped excimer, seems to be detected in the fluorescence as well as in the E-F spectrum. As the temperature decreases, the thermal motion is deactivated, and the molecules trapped with different conformations coexist in the film. One of them with a peak at  $25\,220 \text{ cm}^{-1}$  ( $\sim 396 \text{ nm}$ ), i.e.,  $b_{LT}(I)$ , shows the Stark shift, indicating a large molecular polarizability of the emitting species of  $b_{LT}(I)$ . Two other types of partially overlapped excimer which give  $b_{LT}(II)$  and  $(III)$ , respectively, and the sandwich-type excimer do not show a noticeable Stark shift. Thus, PBA in a PMMA film at a high concentration of 10 mol % shows a plural number of excimer fluorescence emissions which give different electric field effects from each other at low temperatures.

At a low concentration of 0.5 mol %, LE-F increases with a decrease of temperature, as mentioned above. As the temperature decreases, LE-F also increases at a medium concentration, as will be mentioned later. In contrast with those results, the temperature dependence of LE-F at 10 mol % is not significant, though a small increase in intensity is confirmed, as the temperature decreases from 295 to 250 K (see Figure 3a). On the other hand,  $b_{LT}(II)$  increases significantly at 10 mol %, as the temperature decreases. Note that  $b_{LT}(II)$  is not confirmed at 5 mol %, as will be mentioned later. In crystal, the emitting state of the B-fluorescence, i.e., the partially overlapped excimer, is proposed as a precursor of the sandwich-type excimer.<sup>21</sup> The present results imply that the emitting state of  $b_{LT}(II)$  is produced through the LE state in a polymer film; the LE state of PBA may be a precursor of the emitting state of  $b_{LT}(II)$ .

**4.3. At a Medium Concentration of 5 mol %.** Figure 7 shows fluorescence and E-F spectra of PBA in a polymer film at a concentration of 5 mol % observed at different temperatures in the range of 40–295 K. E-F spectra were measured with a field strength of  $1.0 \text{ MV cm}^{-1}$  at 331 nm excitation. In the fluorescence spectra, the sandwich-type excimer fluorescence (EX(1)) with a peak at  $\sim 21\,740 \text{ cm}^{-1}$  (460 nm) is comparable in intensity with the LE-F. The structure of the LE-F, as well as the peak position of EX(1), is independent of the temperature.

At room temperature, E-F spectra of PBA at 5 mol % are similar in shape to the LE-F spectrum in the higher wavenumber region, indicating that the quantum yield of the LE-F becomes lower in the presence of  $F$ . The magnitude of  $\Delta I_F$  at wavenumbers lower than  $21\,000 \text{ cm}^{-1}$  is negligible, implying that EX(1) is not affected by  $F$ . The E-F spectrum shows positive intensity at  $24\,000 \text{ cm}^{-1}$  ( $\sim 415 \text{ nm}$ ), indicating that fluorescence with a peak at  $\sim 415 \text{ nm}$  becomes stronger in the presence of  $F$ . By assuming that the E-F spectrum at room temperature is given by a linear combination between the zeroth derivative components of LE-F and the partially overlapped excimer, the spectral shape of the excimer was extracted. The results are

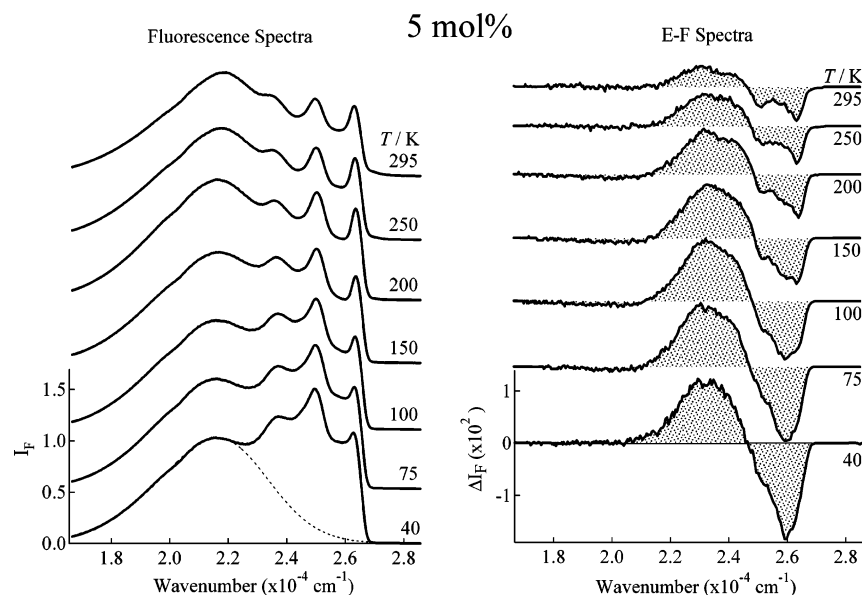


**Figure 7.** Temperature dependence of the fluorescence spectra (left) and the E-F spectra (right) of PBA at a concentration of 5 mol % in a PMMA film. Temperature is shown in each spectrum. Applied field strength was  $1.0 \text{ MV cm}^{-1}$ . A dotted line shows the simulated spectrum of EX(1).

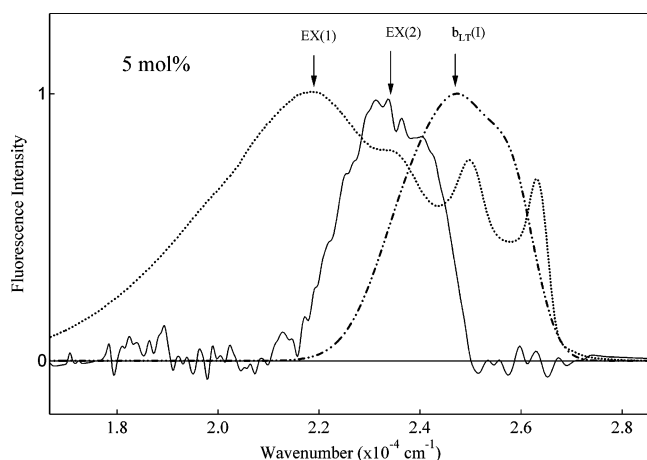


**Figure 8.** Fluorescence spectrum of PBA at 5 mol % (dotted line), EX(2) spectrum at room temperature (solid line), and reextracted fluorescence spectrum at 40 K (chain line).

shown in Figure 8. This excimer corresponds to EX(2) observed at 10 mol %. The field-induced enhancement of the excimer, i.e., EX(2), at 5 mol % probably results from the field-induced increase in the initial population following excitation, as in the case at 10 mol %.

As the temperature decreases,  $I_F$  at  $25\,000 \text{ cm}^{-1}$  markedly increases, which is similar to that at 10 mol % (see Figures 5 and 7). LE-F also increases with a decrease of the temperature, but EX(1) is not so influenced by a change in temperature at 5 mol %. These results show the appearance of emission other than LE-F or EX(1) at 5 mol % at low temperatures. To obtain the spectrum of the newly appearing emission, the spectrum of EX(1) was subtracted from the observed fluorescence spectrum at each temperature in a manner similar to that at 10 mol %. The results of the extracted spectrum are shown in Figure 9a. At room temperature, the extracted spectrum can be regarded as the LE-F (cf. Figures 9a and 1). At low temperatures, on the other hand, the extracted spectra are regarded as a sum of the spectra of LE-F and the newly appearing emission. Then, the extracted spectrum at 295 K was subtracted from the extracted spectrum at 40 K in the manner that the vibrational structure of LE-F disappeared. The reextracted spectrum at 40 K is shown in Figure 9b. By this analysis, it was confirmed that LE-F

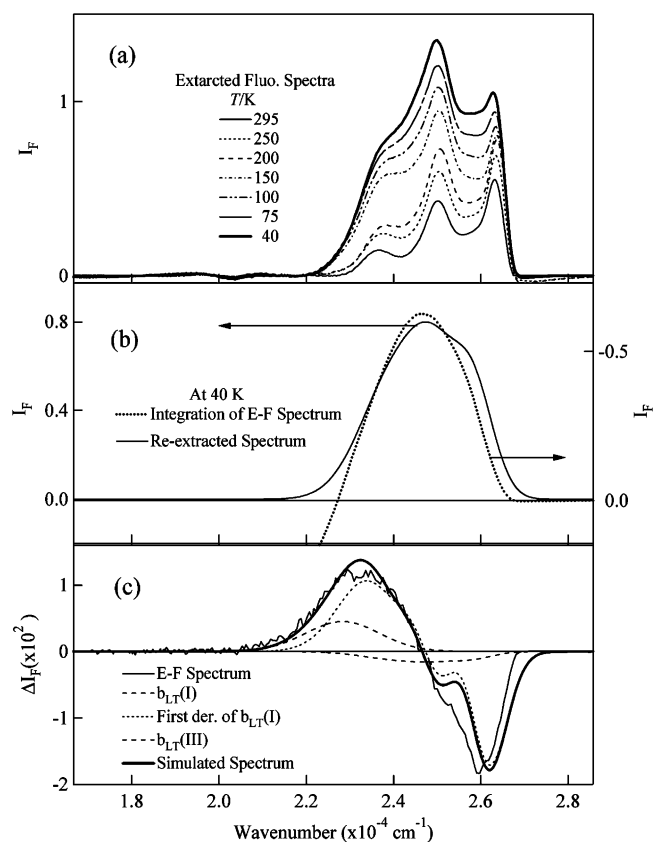


**Figure 9.** (a) Temperature dependence of the extracted fluorescence spectrum of PBA at 5 mol %, (b) reextracted fluorescence spectrum at 40 K (thin solid line) and the integrated spectrum of the E-F spectrum made from the high wavenumber side (dotted line), and (c) E-F spectrum at 40 K (thin solid line), simulated spectrum (thick solid line),  $b_{LT}(I)$  and  $b_{LT}(III)$  having a Gaussian profile (broken lines), and the first derivative of  $b_{LT}(I)$  (dotted line). The simulation in panel b was made by a linear combination of  $b_{LT}(I)$  and  $b_{LT}(III)$  and the first derivative of  $b_{LT}(I)$ .

increases with a decrease of temperature, which probably comes from the temperature dependence of the intramolecular relaxation process of PBA, not from the temperature dependence of the intermolecular process. Note that LE-F increases with a

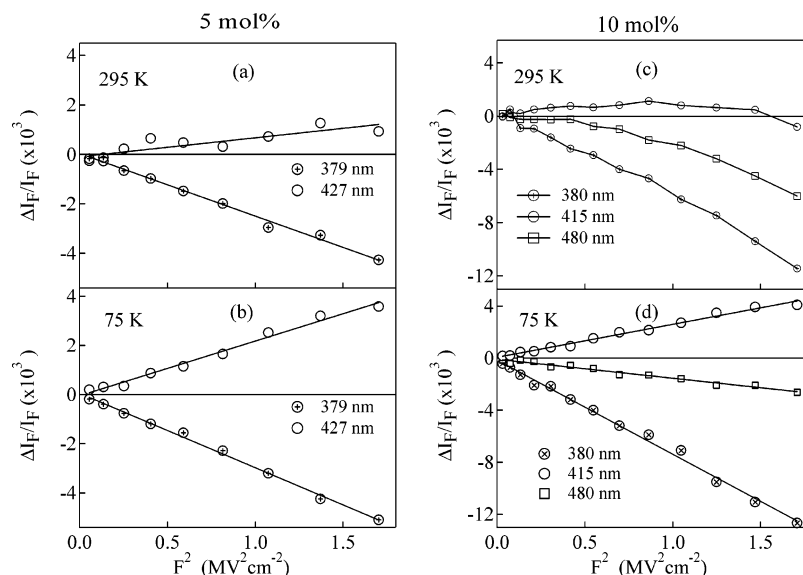


**Figure 10.** Plots of  $\Delta I_F/I_F$  as a function of the square of the applied field strength at different monitoring wavelengths for PBA at 10 (right) and 5 mol % (left) in a PMMA film. Photoexcitation was made at 332 nm for the 10 mol % sample and at 331 nm for the 5 mol % sample.

decrease of temperature at 0.5 mol %, where the intermolecular process is negligible.

E-F spectra of PBA at 5 mol % show a very sharp negative band with a peak at  $\sim 387$  nm and a positive band with a peak at 425 nm at low temperatures. The former band can be attributed neither to the zeroth derivative component of LE-F nor to the first or second derivative component of LE-F. The shape of the E-F spectra reminds us of the first derivative of the broad band with a peak at around  $25\,000\text{ cm}^{-1}$ . The integrated spectrum of the E-F spectrum over the full region is similar to the fluorescence spectrum that newly appears at low temperatures (see Figure 9b). Therefore, it is concluded that fluorescence emission, which is different from EX(1) or EX(2) and shows a remarkable electric field effect at low temperatures, newly appears at low temperatures even at 5 mol %. The fact that the reextracted fluorescence spectrum shown in Figure 9b is similar to the integrated spectrum of the E-F spectrum indicates that the new excimer exhibits the large Stark shift resulting from the change in molecular polarizability between the emitting state and the ground state. In that sense, the fluorescence band that appears at 5 mol % at low temperatures corresponds to the  $b_{LT}(I)$  observed at 10 mol %. Actually, the E-F spectrum at 5 mol % at 40 K could be largely reproduced by combining  $b_{LT}(I)$  with  $b_{LT}(III)$  observed at 10 mol %, i.e., by a linear combination of the zeroth derivative of  $b_{LT}(I)$  and  $b_{LT}(III)$  and the first derivative of  $b_{LT}(I)$ , as shown in Figure 9c. At a medium concentration of 5 mol %, therefore, four emission components, i.e., LE-F, EX(1),  $b_{LT}(I)$ , and  $b_{LT}(III)$ , have been confirmed at low temperatures, while LE-F, EX(1), and EX(2) have been confirmed at room temperature. These fluorescence components are shown in Figure 8. As in the case at 10 mol %,  $b_{LT}(III)$  may correspond to EX(2) confirmed at room temperature in the sense that both are remarkably enhanced by  $F$ . The absence of  $b_{LT}(II)$  and the remarkable temperature dependence of LE-F are very characteristic at 5 mol %, in comparison with the results at 10 mol %. The fact that the presence of  $b_{LT}(II)$  and the temperature dependence of LE-F well depend on the concentration of PBA in a polymer film may suggest that the emitting state of  $b_{LT}(II)$  is produced through the LE state. With respect to these problems, however, further studies will be necessary.

Temperature dependence both of the fluorescence spectrum and of the E-F spectrum has been similarly examined for pyrene in a PMMA film at a concentration of 10 mol %, as preliminarily reported in our previous paper.<sup>15</sup> Pyrene also shows three components of the partially overlapped excimer: bands (I), (II), and (III) with a peak at 393, 415, and 430 nm, respectively, which correspond to  $b_{LT}(I)$ ,  $-(II)$ , and  $-(III)$  in PBA, respectively. Band (I) of pyrene shows the Stark shift, as in the case of  $b_{LT}(I)$ , but the magnitude of the shift is larger in pyrene than that in PBA; the magnitude of the change in molecular polarizability following emission is about two times larger in pyrene ( $250\text{ Å}^3$ ) than in PBA ( $124\text{ Å}^3$ ). In pyrene, band (II), which corresponds to  $b_{LT}(II)$  of PBA and is enhanced with a lowering of the temperature, is not influenced by  $F$  significantly. As a result, band (II) does not appear in the E-F spectra of pyrene at low temperatures. On the other hand,  $b_{LT}(II)$  of PBA appears both in fluorescence spectra and in E-F spectra at low temperatures, indicating that  $b_{LT}(II)$  of PBA is enhanced by  $F$ , in contrast with pyrene.

Finally, the applied field strength dependence of the magnitude of  $\Delta I_F$  has been discussed. In pyrene,  $\Delta I_F$  is proportional to the square of the applied field strength at any monitoring wavelength irrespective of concentration.<sup>16</sup> On the other hand, EX(1) of the methylene-linked compound of pyrene, i.e., 1,3-bis(1-pyrenyl)propane, shows a different electric field effect from that of pyrene; the magnitude of the quenching of EX(1) of the linked compound of pyrene is proportional to the fourth power of the applied field strength at high concentrations in PMMA.<sup>33</sup> It was also found that the linked compound shows a very efficient electroluminescence even in a polymer film, whose spectrum is very similar to that of EX(1). Thus, the applied field strength dependence of photoluminescence (emission induced by photoirradiation) is strongly related to the generation efficiency of electroluminescence in some cases. Therefore, the field strength dependence of the magnitude of the field-induced change in fluorescence intensity of PBA has been measured at several wavelengths and at various temperatures at 5 and 10 mol % in PMMA. At 5 mol %,  $\Delta I_F$  is proportional to the square of the applied field strength at any monitoring wavelength irrespective of temperature, as shown in Figure 10. At 10 mol %,  $\Delta I_F$  is also proportional to the square of the applied field



strength at low temperatures. At room temperature, however,  $\Delta I_F$  of PBA at 10 mol % is not proportional to the square of the applied field strength, as shown in Figure 10c; the magnitude of the quenching at 26 320  $\text{cm}^{-1}$  (380 nm) and 20 830  $\text{cm}^{-1}$  (480 nm) is much larger than that expected for the one that is proportional to the square of the applied field strength. At 24 040  $\text{cm}^{-1}$  (415 nm), which corresponds to a peak position of EX-(2), the field-induced enhancement changes to a field-induced quenching, as the applied field strength becomes larger. To understand the field strength dependence at different monitoring wavelengths, it is important to note that EX(1) is dominant at 10 mol %, and this emission component is superimposed even at 26 320 or 24 040  $\text{cm}^{-1}$ . In analogy with the results of 1,3-bis(1-pyrenyl)propane,<sup>33</sup> it is concluded that EX(1) of PBA shows more efficient field-induced quenching than that expected from the square field strength dependence, and the deviation of  $\Delta I_F$  from the square dependence at 26 320 or 24 040  $\text{cm}^{-1}$  is attributed to the overlap of EX(1) at these monitoring wavenumbers. The efficient field-induced quenching may result from an efficient mobility of hole or electron generated among PBA at high fields, which is necessary for the efficient electroluminescence device. The observation of the clear temperature dependence of the field strength dependence of  $\Delta I_F$  of EX(1) suggests that the hole or electron mobility among PBA is a thermal process, not a tunneling process.

## 5. Conclusion

Remarkable temperature dependence was observed in fluorescence spectra as well as in E-F spectra of PBA in a PMMA film at high and medium concentrations, whereas fluorescence and E-F spectra at a low concentration of PBA where only the LE-F is observed are independent of temperature except for the intensity. LE-F shows the Stark shift in the presence of  $F$  at a low concentration of 0.5 mol %, which results from the difference in molecular polarizability between the LE emitting state and the ground state. At a medium concentration of 5 mol % where LE-F is comparable in intensity to EX(1), EX(1) is not influenced by  $F$  at any temperature, while LE-F and EX(2) are reduced and enhanced by  $F$ , respectively, at room temperature. Excimer fluorescence that shows the remarkable Stark shift newly appears, i.e.,  $b_{LT}(I)$ , as the temperature decreases. At a high concentration of 10 mol % where EX(1) is dominant, other excimer fluorescence emissions, i.e.,  $b_{LT}(II)$  and  $b_{LT}(III)$ , are confirmed at low temperatures, in addition to LE-F, EX(1), and  $b_{LT}(I)$ . LE-F and EX(1) are quenched by  $F$ , while  $b_{LT}(III)$  is enhanced by  $F$ . Among  $b_{LT}(I)$ – $b_{LT}(III)$  observed at low temperatures,  $b_{LT}(I)$  shows both the remarkable Stark shift and the small quenching in the presence of  $F$ , and the others show an enhancement in the presence of  $F$ . Thus, it is concluded that at least five fluorescence components which show different electric field effects from each other exist at high concentrations at low temperatures. The presence of  $b_{LT}(II)$  and the temperature dependence of LE-F well depend on the concentration of PBA in a polymer film, suggesting that the emitting state of  $b_{LT}(II)$  is produced through the LE state.

**Acknowledgment.** This work was supported by Grant-in-Aid for Scientific Research (A) (No. 15205001) and for Scientific Research on Priority Area (417) from the Ministry of Education, Culture, Sports, and Science & Technology of Japan.

## References and Notes

- (1) de Silva, A. P.; Gunaratne, H. Q. N.; Gunnlaugsson, T.; Huxley, A. J. M.; McCoy, C. P.; Rademacher, J. T.; Rice, T. E. *Chem. Rev.* **1997**, 97, 1515 and references therein.
- (2) Winnik, F. M. *Chem. Rev.* **1997**, 93, 587.
- (3) Birks, J. B. *Photophysics of Aromatic Molecules*; Wiley/Interscience: New York, 1970; Chapter 7.
- (4) Kalyanasundaram, K.; Thomas, J. K. *J. Am. Chem. Soc.* **1977**, 99, 2039.
- (5) Deumie, M.; Baraka, M. E.; Quinones, E. *J. Photochem. Photobiol. A: Chem.* **1995**, 87, 105.
- (6) Gratzel, M.; Kalyanasundaram, K.; Thomas, J. K. *J. Am. Chem. Soc.* **1974**, 96, 7869.
- (7) Hrdlovic, P.; Chmela, S. *J. Photochem. Photobiol. A: Chem.* **1997**, 105, 83.
- (8) Ishiji, T.; Kaneko, M. *Analyst* **1995**, 120, 1633.
- (9) Pan, B.; Chakraborty, R.; Berglund, K. A. *J. Cryst. Growth* **1993**, 130, 587.
- (10) Hsiao, J.-S.; Webber, S. E. *J. Phys. Chem.* **1993**, 97, 8289.
- (11) Knopp, J. A.; Weber, G. *J. Biol. Chem.* **1969**, 244, 6309.
- (12) Prodi, L.; Ballardini, R.; Gandolfi, M. T.; Roversi, R. *J. Photochem. Photobiol. A: Chem.* **2000**, 136, 49.
- (13) Bordonaro, J. L.; Curtis, W. R. *Biotechnol. Bioeng.* **2000**, 70, 176.
- (14) Schneider, I.-M.; Dobner, B.; Neubert, R.; Wohlrab, W. *Int. J. Pharm.* **1996**, 145, 187.
- (15) Iimori, T.; Ara, A. M.; Yoshizawa, T.; Nakabayashi, T.; Ohta, N. *Chem. Phys. Lett.* **2005**, 402, 206.
- (16) Ohta, N.; Umeuchi, S.; Kanada, T.; Nishimura, Y.; Yamazaki, I. *Chem. Phys. Lett.* **1997**, 279, 215.
- (17) Umeuchi, S.; Nishimura, Y.; Yamazaki, I.; Murakami, H.; Yamashita, M.; Ohta, N. *Thin Solid Films* **1997**, 311, 239.
- (18) Ohta, N. *Bull. Chem. Soc. Jpn.* **2002**, 75, 1637.
- (19) Bublit, G. U.; Boxer, S. G. *Annu. Rev. Phys. Chem.* **1997**, 48, 213.
- (20) Locknar, S. A.; Peteanu, L. A. *J. Phys. Chem. B* **1998**, 102, 4240.
- (21) Mizuno, K.; Matsui, A. *J. Lumin.* **1987**, 38, 323.
- (22) Matsui, A.; Ohno, T.; Mizuno, K.; Yokoyama, T.; Kobayashi, M. *Chem. Phys.* **1987**, 111, 121.
- (23) Matsui, A.; Mizuno, K.; Tamai, N.; Yamazaki, I. *Chem. Phys.* **1987**, 113, 111.
- (24) Seyfang, R.; Port, H.; Fischer, P.; Wolf, H. C. *J. Lumin.* **1992**, 51, 197.
- (25) Nakabayashi, T.; Morikawa, T.; Ohta, N. *Chem. Phys. Lett.* **2004**, 395, 346.
- (26) Bottcher, C. J. F.; Bordewijk, P. *Theory of Electronic Polarization*; Elsevier: Amsterdam, The Netherlands, 1978; Vol. 1.
- (27) Taniguchi, Y.; Mitsuya, M.; Tamai, N.; Yamazaki, I.; Masuhara, H. *Chem. Phys. Lett.* **1986**, 132, 516.
- (28) Seyfang, R.; Betz, E.; Port, H.; Schrof, W.; Wolf, H. C. *J. Lumin.* **1985**, 34, 57.
- (29) Ohta, N.; Umeuchi, S.; Kanada, T.; Akita, K.; Kawabata, H.; Yamazaki, I. *J. Lumin.* **2000**, 87–89, 733.
- (30) Horiguchi, R.; Iwasaki, N.; Maruyama, Y. *J. Phys. Chem.* **1987**, 91, 5135.
- (31) Yamanaka, T.; Takahashi, Y.; Kitamura, T.; Uchida, K. *J. Lumin.* **1991**, 48 and 49, 265.
- (32) Sumi, H. *Chem. Phys.* **1989**, 130, 433.
- (33) Ohta, N.; Kawabata, H.; Umeuchi, S.; Yamazaki, I. *Chem. Phys. Lett.* **1999**, 310, 397; **1999**, 315, 151.